Dielectric tensor and shear-mode dispersion for strongly coupled Coulomb liquids: Three-dimensional one-component plasmas

Kenneth I. Golden
Department of Computer Science and Electrical Engineering, University of Vermont, Burlington, Vermont 05405

G. Kalman
Department of Physics, Boston College, Chestnut Hill, Massachusetts 02167

Philippe Wyns
Hewlett-Packard, Colorado Integrated Circuits Division, Mail Stop 64, 3404 East Harmony Road, Fort Collins, Colorado 80525
(Received 21 January 1991; revised manuscript received 15 June 1992)

We analyze the transverse dielectric response function and the collective excitations in a strongly coupled one-component plasma (OCP). The collective modes are either photonlike or phononlike. The latter, which are maintained by shear, are unique to the strongly coupled system. We employ the recently established quasilocalized-charge model to develop a theory of the shear mode in the strongly coupled OCP. We examine in detail the dispersion of the shear mode in the $20<\Gamma<225$ domain, including the supercooled liquid state ($\Gamma=Z^2e^2/ak_BT$, a is the Wigner-Seitz radius), and compare it with the result of molecular-dynamics simulations of Hansen, McDonald, and Pollock [Phys. Rev. A **11**, 1025 (1975)]. The agreement between the theory and the simulation results is quite satisfactory in the low-k domain, but the theory is unable to account for the observed high-k splitting of the shear mode. We also establish the correspondence between the shear mode of the strongly coupled OCP liquid and the acoustic phonons of the Wigner crystal.

PACS number(s): 52.25.Mq, 52.35.Lv

I. INTRODUCTION

This is the fourth in a series of papers [1–3] (to be referred to as Papers I, II, III, respectively), which thus far have concentrated on the formulation of the longitudinal dielectric-response function and on the concomitant problem of plasmon dispersion in a variety of strongly coupled Coulomb liquids. The longitudinal plasmon excitation constitutes, however, only part of the full collective excitation spectrum for such systems. The other major component of the excitation spectrum comprises the transverse modes. The transverse modes are either photonlike (i.e., they represent transverse electromagnetic waves slightly modified by the presence of the medium) or phononlike (i.e., they are maintained by particle-particle interactions and survive even in the $c\rightarrow\infty$ limit). The transverse excitations are the shear waves, whose existence in crystal lattices relates to the fundamental properties of solids; they are also known to exist in dense neutral liquids, albeit in a restricted-wave-number (k) domain, excluding the $k\rightarrow 0$ region. As to Coulomb systems, shear waves (transverse phonons) in Wigner crystals (both in three and two dimensions) have been analyzed theoretically, and their occurrence in strongly coupled Coulomb liquids (again, both in three and two dimensions) has been predicted on the basis of molecular-dynamics (MD) computer simulations as discussed in greater detail below. In contrast to the longitudinal plasmon mode, the transverse shear mode is a *prima facie* correlational effect, which obviously does not exist in a weakly coupled plasma or liquid. It is the periodic or quasiperiodic arrangement of the particles induced by strong correlations that is responsible for the ability of the system to maintain shear. Thus the description of shear waves in the one-component plasma (OCP) is possible only with the aid of a formalism that can handle strong correlations. Such a formalism has been worked out in our earlier works [1–3]. The study of the dispersion characteristics of shear waves in simple strongly coupled Coulomb liquids, on the basis of the theoretical model introduced earlier [1] and used for the analysis of the plasmon mode [2,3], is the principal objective of the present and the following paper. As such, it is to provide a theoretical model, based on first principles, for shear-mode propagation in strongly coupled Coulomb liquids.

From a more formal point of view, the longitudinal dielectric-response function is only a part of the full dielectric-response tensor that normally has six independent elements when the (three-dimensional) system is pervaded by an external dc magnetic field. When an external magnetic field is absent—which is the situation in the present paper—the plasma is isotropic and the dielectric tensor has only two independent elements, the longitudinal and transverse (with respect to the wave vector $\mathbf{k}$) elements. In contrast to what was done in Papers I, II, and III, we now focus on the properties of the transverse element of the dielectric tensor.

Yet another point of view is provided by observing that the analysis of the transverse modes or of the transverse response requires the inclusion of the full (longitudinal and transverse) interaction in the equation of motion,

even though it is only the longitudinal interaction that is responsible for the excitation of the shear waves. In Papers I, II, and III, we considered only Coulomb interactions and we calculated the linear response of the system to an external scalar potential perturbation. In this paper, we go further: we include the full self-consistent electromagnetic response in the microscopic equations of motion and we calculate the linear response to combined external scalar and vector potential perturbations. As a result, the scalar response formalism of Paper I is generalized to a response *tensor* formalism and we are led to the self-consistent formulation of the calculation of the transverse response in this approximation.

The system we address in this paper is the uniform background classical three-dimensional (3D) OCP. The strength of the coupling in the OCP is characterized by the coupling parameter $\Gamma=\beta(Ze)^2/a$, where $\beta^{-1}=k_B T$ is the thermal energy per particle and a is the Wigner-Seitz radius $(4\pi/3)a^3 n=1$. Monte Carlo simulations indicate that the OCP crystallizes into a bcc lattice at $\Gamma_m=178\pm1$.

Theoretical calculations of shear-mode (acoustic-phonon) dispersion in the 3D bcc Wigner lattice have traced the $\omega(\mathbf{k})$ dispersion curve for a number of principal directions up to the Brillouin-zone boundary [4] and for arbitrary directions in the small-k limit [5]. In a real metallic lattice the electronic screening affects the small-k portion of the dispersion curve: with these modifications, computations for the bcc lattice of sodium were carried out some time ago by a number of investigators [6] and rather good agreement with the experimental data of Woods *et al.* [7] was obtained. As to the question of whether 3D Coulomb liquids ($\Gamma<\Gamma_m$) can sustain the transverse shear mode, evidence of well-defined shear modes in the strongly coupled ionic OCP was reported by Hansen, McDonald, and Pollock [8] in their molecular-dynamics (MD) computer simulations for $\Gamma=152.4$, which is, however, still well above the melting temperature.

The observation that serves as the basis of the formal development presented both in Paper I and in this paper, is that the dominating feature of the physical state of a plasma with $\Gamma\gg1$ is the quasilocalization of the charges. This physical picture leads to a model—the quasilocalized-charge (QLC) model—which resembles that of a disordered solid where the particles occupy randomly located sites and undergo small-amplitude oscillations around them. At the same time, however, the site positions also slowly change and a continuous rearrangement of the quasiequilibrium configuration takes place. Nevertheless, inherent in the model is the assumption that the two time scales are well separated; consequently, in the description of the fast oscillating motions, the time average (converted into ensemble average) of the drifting quasiequilibrium configuration is sufficient. This condition can be formulated as $\omega\tau_D>1$, where τ_D is the "diffusion time" of the quasisites. The assumption that this condition is satisfied is quite reasonable for the high-frequency 3D plasmon mode. The shear mode, however, has an acoustic-type dispersion ($\omega\propto k$), and thus the condition is bound to exclude a $k<k_{\min}$ domain, where $k_{\min}$ is determined by τ_D. Since correlations are crucial for the maintenance of the shear mode and we argue that the correlations break down over the period of the oscillation if $k<k_{\min}$, we can conclude that the shear mode does not propagate in this domain. The assertion that the $\omega\tau_D\gg1$ condition is violated for $k<k_{\min}$ and the ensuing conclusion are just a restatement of the well-known fact that while in a solid the shear mode is well defined down to $k=0$, in a liquid it exists only for finite k.

The QLC model describes the motions of the system around the average configuration represented through the equilibrium pair-correlation function, which, in turn, reflects the effect of the temperature on the probability of the various microstates. We have referred to this [1–3] as the "indirect thermal effect" to distinguish it from the "direct thermal effect," which represents the slow diffusion and migration of the quasisites. Even though the latter is not described by the primitive QLC model, we have been able to provide a satisfactory phenomenological treatment of some of its aspects by recasting the QLC formalism in a static-mean-field-theory (MFT) language. This method has been used in Paper II to successfully predict the behavior of the plasmon dispersion in a two-dimensional OCP. This approach is able to handle the high-k modifications of the dispersion (mainly due to thermal motion and Landau damping) but is not able to describe the low-k effect (due mainly to the disruption of correlations because of site migration and collisional damping).

The plan of this paper is as follows: In Sec. II, we establish the QLC microscopic equation-of-motion basis for the calculation of the linear response to small external scalar and vector potential perturbations; straightforward calculations of the density and current response and of the dielectric-response tensor follow. The results of Sec. II are applied to Sec. III, where we calculate the dispersion of the transverse—both electromagnetic and shear—modes. We compare our calculated QLC shear-mode oscillation frequency with MD data, and we show the correspondence with results pertaining to transverse phonon dispersion in the 3D bcc Wigner lattice and also with experimental data for the sodium bcc lattice. In Sec. IV, we incorporate the direct thermal effect in the response tensor by reformulating it into a mean-field-theory expression. We then recalculate the shear-mode dispersion and Landau damping rate and again compare with the MD data. Conclusions are drawn in Sec. V.

II. RESPONSE AND DIELECTRIC TENSOR

In this section we apply the QLC approach of Paper I to the calculation of the dynamical matrix and of the full dielectric-response tensor for the strongly coupled OCP.

The OCP consists of N particles, each of mass m and carrying charge Ze, embedded in a neutralizing uniform background of N_b particles, each carrying charge $Z_b e$. Overall charge neutrality requires that $N_b Z_b+NZ=0$. The OCP plasma frequency is given by $\omega_p=(4\pi Z^2 e^2 n/m)^{1/2}$, where $n=N/V$ is the unperturbed density of plasma particles.

We wish to calculate the linear response to small per-

turbing external *scalar* and *vector* potentials $\hat{\Phi}$ and $\hat{\mathbf{A}}$. Following the QLC approach of Paper I, we consider the microscopic equations of motion describing the rapid oscillations of the charges about their slowly drifting equilibrium site positions. As explained in the Introduction, the QLC approximation amounts to neglecting the "direct" thermal effect against correlational effects, which for $\Gamma \gg 1$ is a good approximation since the former is $O(\Gamma^{-1})$ times the latter. Let now $X_{i,\mu}(t)=x_{i,\mu}+\xi_{i\mu}(t)$ be the momentary position of the ith particle, $x_{i,\mu}$ its quasiequilibrium site position, and $\xi_{i,\mu}$ the perturbed amplitude of its small excursion [i,j enumerate particles and μ,ν are three-dimensional vector indices; Einstein summation convention for the repeated indices is understood; we use the Coulomb gauge where $\mathbf{E}_L=-\nabla\Phi$, and $\mathbf{E}_T=-(1/c)\dot{\mathbf{A}}$; L and T subscripts refer to longitudinal and transverse elements or components]. The microscopic equation of motion of the ith particle is

$$-m\omega^2\xi_{i,\mu}(\omega)+\sum_j K_{ij,\mu\nu}\xi_{j,\nu}(\omega) = \frac{i\omega}{c}ZeA_\mu(\mathbf{x}_i,\omega)+Ze\hat{E}_\mu(\mathbf{x}_i,\omega)\ , \tag{1}$$

where $\hat{E}_\mu(\mathbf{x}_i,\omega)=(i\omega/c)\hat{A}_\mu(\mathbf{x}_i,\omega)-(\partial/\partial x_{i,\mu})\hat{\Phi}(\mathbf{x}_i,\omega)$ is the full external electric-field perturbation; from Paper I, $K_{ij,\mu\nu}$ for the 3D OCP is calculated to be

$$K_{ij,\mu\nu}=\frac{Z^2}{V}\sum_{\mathbf{q}} q_\mu q_\nu\phi(q)\{e^{i\mathbf{q}\cdot(\mathbf{x}_i-\mathbf{x}_j)}-\delta_{ij}e^{i\mathbf{q}\cdot\mathbf{x}_i}n_{\mathbf{q}}+\delta_{ij}N\delta_{\mathbf{q}}\}\ , \tag{2}$$

where $\phi(q)=4\pi e^2/q^2$ is the Fourier transform of the Coulomb potential $\phi(r)=e^2/r$; the unperturbed ("base") microscopic density, $n_{\mathbf{q}}=\sum_j e^{-i\mathbf{q}\cdot\mathbf{x}_j}$ depends on the $\mathbf{x}_i$, $\mathbf{x}_j$, etc., which are the coordinates of the random sites and are not dynamical variables. The force term in (1) now includes, in addition to $K_{ij,\mu\nu}$, the vector potential $\mathbf{A}$, which depends on the current sources originating from all the other moving charges labeled $j\,(j\neq i)$, i.e.,

$$A_\mu(\mathbf{x}_i,\omega)=-\frac{4\pi}{c}Ze\sum_j(1-\delta_{ij})i\omega\xi_{j,\nu}(\omega)\frac{1}{V} \times\sum_{\mathbf{q}}T_{\mu\nu}(\mathbf{q})\frac{1}{q^2-(\omega/c)^2}e^{i\mathbf{q}\cdot(\mathbf{x}_i-\mathbf{x}_j)}\ , \tag{3}$$

where $T_{\mu\nu}(\mathbf{q})=\delta_{\mu\nu}-q_\mu q_\nu/q^2$ is the transverse projection tensor.

We next introduce the collective coordinates $\xi_{\mathbf{q},\mu}$ via the Fourier representation

$$\xi_i(\omega)=\frac{1}{\sqrt{Nm}}\sum_{\mathbf{q}}\xi_{\mathbf{q}}(\omega)e^{i\mathbf{q}\cdot\mathbf{x}_i} \tag{4}$$

and carry out the algebraic operations of Paper I. The principal assumption of the QLC approach consists of replacing the random $\mathbf{x}_i$, $\mathbf{x}_j$, etc. base coordinates everywhere in the resulting microscopic equation of motion for $\xi_{\mathbf{q}}(\omega)$ by their ensemble average. This latter is evaluated through

$$\begin{aligned}
&\langle n_{\mathbf{p}}\rangle=N\delta_{\mathbf{p}}\ ,\\
&\langle n_{\mathbf{p}}n_{\mathbf{q}}\rangle=N\delta_{\mathbf{p}+\mathbf{q}}\{1+ng(q)+N\delta_{\mathbf{q}}\}\ ,\\
&\langle e^{-i\mathbf{p}\cdot\mathbf{x}_i}e^{-i\mathbf{q}\cdot\mathbf{x}_j}\rangle|_{i\neq j}=\frac{1}{N-1}\delta_{\mathbf{p}+\mathbf{q}}\{ng(q)+N\delta_{\mathbf{q}}\}\ ,
\end{aligned} \tag{5}$$

where $g(q)$ is the Fourier transform of the equilibrium pair-correlation function $g(r)$. The equation of motion that results from this procedure (cf. Paper I) is

$$\{\omega^2\delta_{\mu\nu}-C_{\mu\nu}(\mathbf{k}\omega)\}\xi_{\mathbf{k},\nu}(\omega)=-\frac{Zen}{\sqrt{Nm}}\hat{E}_\mu(\mathbf{k}\omega)\ , \tag{6}$$

where the dynamical matrix $\underline{C}$ is given by

$$C_{\mu\nu}(\mathbf{k}\omega)=\omega_p^2\{L_{\mu\nu}(\mathbf{k})+T_{\mu\nu}(\mathbf{k})\frac{\omega^2}{\omega^2-k^2c^2+io} +\mathcal{D}_{\mu\nu}(\mathbf{k})\}+\omega^2\mathcal{Q}_{\mu\nu}(\mathbf{k}\omega)\ , \tag{7}$$

$$\mathcal{D}_{\mu\nu}(\mathbf{k})=\frac{1}{V}\sum_{\mathbf{q}}L_{\mu\nu}(\mathbf{q})\{g(|\mathbf{k}-\mathbf{q}|)-g(q)\}\ , \tag{8}$$

$$\mathcal{Q}_{\mu\nu}(\mathbf{k}\omega)=\frac{1}{V}\sum_{\mathbf{q}}T_{\mu\nu}(\mathbf{q})\frac{\omega_p^2}{\omega^2-q^2c^2+io}g(|\mathbf{k}-\mathbf{q}|)\ . \tag{9}$$

o is the customary infinitesimal small positive quantity, ensuring the causal behavior of the propagators; $L_{\mu\nu}(\mathbf{q})=q_\mu q_\nu/q^2$ is the longitudinal projection tensor. Evidently, the transverse interaction manifests itself through two terms in (7): the term containing $T_{\mu\nu}(\mathbf{k})$ represents the average field, while $\mathcal{Q}_{\mu\nu}$ represents the fluctuating part of the field. This latter, which is relativistically small, has been shown to induce a relativistically small upward shift in the plasma frequency [9]. However, it has no significance from the point of view of the discussion that follows; we therefore set $\mathcal{Q}_{\mu\nu}(\mathbf{k}\omega)=0$ in the sequel.

The calculation of the dielectric-response tensor $\epsilon_{\mu\nu}(\mathbf{k}\omega)$, or, equivalently, of the polarizability tensor $\alpha_{\mu\nu}(\mathbf{k}\omega)\equiv\epsilon_{\mu\nu}(\mathbf{k}\omega)-\delta_{\mu\nu}$ is carried out first by observing that, to lowest order in $\hat{\mathbf{E}}$, the perturbed microscopic density and current density are given by

$$\begin{aligned}
\rho_{\mathbf{k}}(\omega)&=-\frac{ik_\mu}{\sqrt{Nm}}\sum_{\mathbf{q}}n_{\mathbf{k}-\mathbf{q}}\xi_{\mathbf{q},\mu}(\omega)\ ,\\
j_{\mathbf{k},\mu}(\omega)&=-\frac{i\omega}{\sqrt{Nm}}\sum_{\mathbf{q}}n_{\mathbf{k}-\mathbf{q}}\xi_{\mathbf{q},\mu}(\omega)
\end{aligned} \tag{10}$$

[cf. Eq. (4)]. Their equilibrium averages $\rho(\mathbf{k}\omega)\equiv\langle\rho_{\mathbf{k}}(\omega)\rangle$ and $j(\mathbf{k}\omega)\equiv\langle j_{\mathbf{k}}(\omega)\rangle$ can be calculated by averaging only over $n_{\mathbf{k}-\mathbf{q}}$ in (10), since the $\xi_{\mathbf{q}}(\omega),\xi_{\mathbf{p}}(\omega)$, by virtue of the assumption used in deriving (6), are independent of the $\mathbf{x}_i$ coordinates. Substituting (6) into (10) and averaging, we obtain

$$j_\mu(\mathbf{k}\omega)=\frac{i\omega Zen}{m}[\omega^2\underline{I}-\underline{C}(\mathbf{k}\omega)]^{-1}_{\mu\nu}\hat{E}_\nu(\mathbf{k}\omega)\ . \tag{11}$$

The longitudinal response of the system is most conveniently characterized through the "external" and "total" density response functions $\hat{\chi}(\mathbf{k}\omega)$ and $\chi(\mathbf{k}\omega)$, defined by (and augmented by the subscript L)

$$\rho(\mathbf{k}\omega)=\hat{\chi}_L(\mathbf{k}\omega)Ze\hat{\Phi}(\mathbf{k}\omega)$$
$$=\chi_L(\mathbf{k}\omega)Ze[\hat{\Phi}(\mathbf{k}\omega)+\Phi^{\rm ind}(\mathbf{k}\omega)]\ , \tag{12}$$

where $\rho(\mathbf{k}\omega)$ and $\Phi^{\rm ind}(\mathbf{k}\omega)$ are the first-order average density and scalar potential responses to the $\hat{\Phi}$ perturbation. The analog of Eq. (12) for transverse perturbation and response is

$$j_{T\mu}(\mathbf{k}\omega)=\hat{\chi}_T(\mathbf{k}\omega)Zec\,\hat{A}_\mu(\mathbf{k}\omega)$$
$$=\chi_T(\mathbf{k}\omega)Zec[\hat{A}_\mu(\mathbf{k}\omega)+A_\mu^{\rm ind}(\mathbf{k}\omega)]\ . \tag{13}$$

These definitions imply that the scalar potential $\Phi^{\rm ind}$ and the vector potential $\mathbf{A}^{\rm ind}$ are given in the Coulomb gauge. The dielectric tensor $\epsilon_{\mu\nu}(\mathbf{k}\omega)=L_{\mu\nu}(\mathbf{k})\epsilon_L(\mathbf{k}\omega)+T_{\mu\nu}(\mathbf{k})\epsilon_T(\mathbf{k}\omega)$ can now be constructed from χ_L and χ_T as

$$\epsilon_{\mu\nu}(\mathbf{k}\omega)=\delta_{\mu\nu}-\phi(k)\left\{\chi_L(\mathbf{k}\omega)L_{\mu\nu}(\mathbf{k})-\chi_T(\mathbf{k}\omega)\frac{k^2c^2}{\omega^2}T_{\mu\nu}(\mathbf{k})\right\}\ . \tag{14}$$

From Eqs. (11) to (13), one can identify $\hat{\chi}_L$ and $\hat{\chi}_T$ as

$$\hat{\chi}_L(\mathbf{k}\omega)=\frac{nk^2}{m}L_{\mu\nu}(\mathbf{k})[\omega^2\underline{I}-\underline{C}(\mathbf{k}\omega)]^{-1}_{\mu\nu} \tag{15}$$

and

$$\hat{\chi}_T(\mathbf{k}\omega)=\frac{-n\omega^2}{mc^2}T_{\mu\nu}(\mathbf{k})[\omega^2\underline{I}-\underline{C}(\mathbf{k}\omega)]^{-1}_{\mu\nu}\ . \tag{16}$$

Then, using the relationships between $\chi_{L,T}$ and $\hat{\chi}_{L,T}$ as implied by Eqs. (12) and (13),

$$\hat{\chi}_L(\mathbf{k}\omega)=\frac{\chi_L(\mathbf{k}\omega)}{\epsilon_L(\mathbf{k}\omega)}\ , \tag{17}$$

$$\hat{\chi}_T(\mathbf{k}\omega)=\chi_T(\mathbf{k}\omega)\frac{1-\frac{k^2c^2}{\omega^2}}{\epsilon_T(\mathbf{k}\omega)-\frac{k^2c^2}{\omega^2}}\ , \tag{18}$$

one obtains the longitudinal and transverse polarizabilities

$$\alpha_L(\mathbf{k}\omega)=-\frac{\omega_p^2}{\omega^2-\omega_p^2\mathcal{D}_L(\mathbf{k})}\ , \tag{19}$$

$$\alpha_T(\mathbf{k}\omega)=-\frac{\omega_p^2}{\omega^2-\omega_p^2\mathcal{D}_T(\mathbf{k})}\ , \tag{20}$$

$$\mathcal{D}_L(\mathbf{k})=L_{\mu\nu}(\mathbf{k})\mathcal{D}_{\mu\nu}(\mathbf{k})$$
$$=\frac{1}{V}\sum_{\mathbf{q}}\chi^2\{g(|\mathbf{k}-\mathbf{q}|)-g(q)\}$$
$$=-2\int_0^\infty dr\frac{1}{r}g(r)\left\{\frac{\sin kr}{kr}+\frac{3\cos kr}{k^2r^2}-\frac{3\sin kr}{k^3r^3}\right\}\ , \tag{21}$$

$$\mathcal{D}_T(\mathbf{k})=\tfrac{1}{2}T_{\mu\nu}(\mathbf{k})\mathcal{D}_{\mu\nu}(\mathbf{k})$$
$$=-\tfrac{1}{2}\mathcal{D}_L(\mathbf{k})\ , \tag{22}$$

where $\chi\equiv\mathbf{k}\cdot\mathbf{q}/(kq)$.

The expressions (19) and (20) for the longitudinal and transverse elements of the total polarizability tensor obviously satisfy the $\Gamma\gg1$ limits of the exact longitudinal and nonretarded transverse ω^{-4} third-frequency-moment sum rules [8] and their more general retarded sum-rule counterparts [10] in the $c\to\infty$ limit. For $k\to0$, $\mathcal{D}_L(\mathbf{k})$ and $\mathcal{D}_T(\mathbf{k})$ become

$$\mathcal{D}_L(k\to0)=\frac{4}{45}\frac{\beta E_c(\Gamma)}{\Gamma}k^2a^2\ , \tag{23}$$

$$\mathcal{D}_T(k\to0)=-\frac{2}{45}\frac{\beta E_c(\Gamma)}{\Gamma}k^2a^2\ , \tag{24}$$

the coupling-dependent correlation energy per particle $E_c(\Gamma)$ is given by the Stringfellow-DeWitt-Slattery formula [11]

$$\beta E_c(\Gamma)=-0.899\,577\,\Gamma+0.579\,554\,\Gamma^{1/3}-0.251\,460\ . \tag{25}$$

For large k values, $\mathcal{D}_L$ and $\mathcal{D}_T$ reach the asymptotic limits

$$\mathcal{D}_L(k\to\infty)=-\tfrac{2}{3}\ , \tag{26}$$

$$\mathcal{D}_T(k\to\infty)=\tfrac{1}{3}\ . \tag{27}$$

The asymptotic value (26) is in agreement with the exact sum-rule requirement $(\frac{2}{3})g(r=0)$ derived by Shaw [12] and Niklasson [13].

III. QLC DESCRIPTION OF COLLECTIVE MODES

In this section, we calculate the collective-mode dispersions of the transverse excitations and make contact with the dispersion of the shear waves observed in the MD simulations of Hansen, McDonald and Pollock [8] and with the behavior of shear waves in the 3D Wigner lattice [4–6].

Either the dynamical matrix formula (7) or the tensor polarizability formulas (19) and (20) can serve as the starting point for generating the dispersion relations. Only the dispersion of the collective modes but not the damping can be determined from the present QLC approach. As discussed in Papers I and III, collisional damping is absent from such a model because in a strongly coupled Coulomb liquid, particles on different sites are virtually isolated from each other. Plasmon-plasmon-type, plasmon-shear-mode-type, shear-mode-shear-mode-type, interactions are absent because the inherent nonlinearity of the Coulomb interaction is not taken into account in the harmonic approximation underlying the QLC model. The calculation of these various dissipative mechanisms is beyond the scope of the present paper and has to await further work and clarification. As to direct thermal effects and the concomitant Landau damping, they profoundly affect the high-k dispersion of the transverse shear mode. These

effects we will later incorporate into the approximation scheme (in Sec. IV) by reformulating the QLC theory into a mean-field theory.

First a few words about plasmon dispersion in the strongly coupled 3D OCP. In Papers I and III, we calculated the plasmon frequency from the corresponding QLC formula for the longitudinal dielectric function. This calculation is readily reproduced in the present work by setting $\omega^2=C_L(\mathbf{k}\omega)$ [$C_L(\mathbf{k}\omega)$ is the longitudinal element of the dynamical matrix (7)]. The plasmon frequency

$$\omega(\mathbf{k})=\omega_p\{1+\mathcal{D}_L(\mathbf{k})\}^{1/2} , \tag{28}$$

which result is shown as the upper curve in Fig. 1. We note from (26) that the plasmon frequency tends to the asymptotic value $\omega(\infty)=\omega_p/\sqrt{3}$. More will be said about this limit below.

Turning now to the dispersion of the transverse collective modes, the collective-mode frequency $\omega(\mathbf{k})$ is calculated either by setting $\omega^2=C_T(\mathbf{k}\omega)$ [$C_T(\mathbf{k}\omega)$ is the transverse projection of the dynamical matrix (7)] or from the transverse dispersion relation

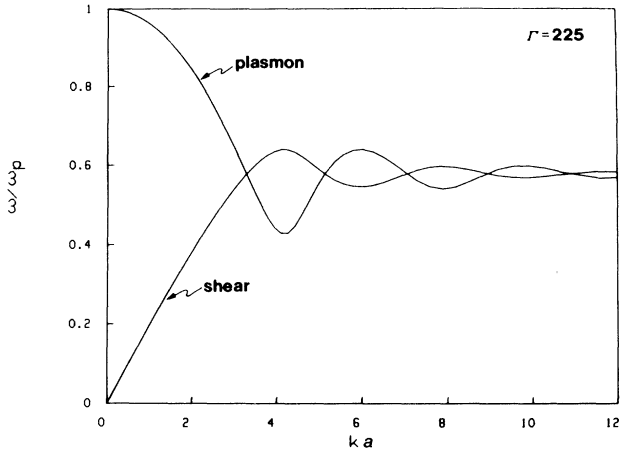

FIG. 1. Transverse shear-mode [calculated from QLC Eq. (32)] and longitudinal plasmon dispersion curves (from Ref. [3]) for $\Gamma=225$.

$$\frac{k^2c^2}{\omega^2}=\epsilon_T(\mathbf{k}\omega)=1+\alpha_T(\mathbf{k}\omega) , \tag{29}$$

where $\alpha_T(\mathbf{k}\omega)$ is given by (20). The two solutions of (29) are

$$\omega^2(\mathbf{k})=\tfrac{1}{2}\{\omega_p^2[1+\mathcal{D}_T(\mathbf{k})]+k^2c^2\pm\sqrt{(\omega_p^2[1+\mathcal{D}_T(\mathbf{k})]+k^2c^2)^2-4\omega_p^2k^2c^2\mathcal{D}_T(\mathbf{k})}\} . \tag{30}$$

Equation (30) comprises the high-frequency electromagnetic and low-frequency shear modes. In the $k\to 0$ limit they become, respectively,

$$\omega^2(\mathbf{k})=\begin{cases}\omega_p^2[1+\mathcal{D}_T(\mathbf{k})]+k^2c^2\\ k^2c^2\mathcal{D}_T(\mathbf{k}) .\end{cases} \tag{31}$$

This limit holds only in the small wave-number domain $kc\ll\omega_p$. For any reasonable k value, the opposite limit $kc\gg\omega_p$, prevails. In this case,

$$\omega^2(\mathbf{k})=\begin{cases}\omega_p^2+k^2c^2 \quad \text{(electromagnetic)}\\ \omega_p^2\mathcal{D}_T(\mathbf{k}) \quad \text{(shear)} .\end{cases} \tag{32}$$

The electromagnetic mode is the equivalent of the transverse polariton mode in the Wigner crystal; the shear-mode relation can be obtained directly from Eq. (29) by letting c go to infinity and requiring that $\epsilon_T^{-1}(\mathbf{k}\omega)=0$. As expected, correlational effects originating from $\mathcal{D}_T(\mathbf{k})$ are virtually undetectable in the electromagnetic mode dispersion.

For the analysis of the shear mode, the three wave-number domains

$$\begin{aligned}&(ka)^2\ll 3\Gamma/(\beta mc^2)\ll 1 ,\\ &3\Gamma/(\beta mc^2)\ll(ka)^2\ll 1 ,\\ &(ka)^2\gg 1 ,\end{aligned} \tag{33}$$

have to be distinguished. The analysis of (31) in the first domain gives

$$\omega(\mathbf{k})=kc\sqrt{\mathcal{D}_T}=k^2ac\left[\frac{2}{45}\frac{\beta|E_c(\Gamma)|}{\Gamma}\right]^{1/2} . \tag{34}$$

Note that $\omega\propto k^2$ in this domain. Earlier we have argued, however, that shear waves cannot propagate at such long wavelengths since diffusion of the quasisites (a mechanism not included in the present QLC formalism) occurs over times much shorter than the shear-mode oscillation time $\sim(kc\sqrt{\mathcal{D}_T})^{-1}$ inferred from (34) above; thus, the quasisite diffusion completely disrupts the large-scale order needed to sustain the shear mode at small wave numbers. Equation (34) is therefore of academic interest only.

The second and third domains [corresponding to $(kc/\omega_p)^2\gg 1$] are far more significant insofar as shear-mode dispersion is concerned. A glance at (32) reveals that in the second domain the shear mode exhibits an acoustic behavior

$$\omega(\mathbf{k})=kV_0(\Gamma) \tag{35}$$

with the shear velocity

$$V_0(\Gamma)=\sqrt{\tfrac{2}{15}[|E_c(\Gamma)|/m]} , \tag{36}$$

which is of the order $\sqrt{\Gamma}$ times the thermal velocity. In the third domain, (27) and (32) provide

$$\omega(k\to\infty)\to\frac{\omega_p}{\sqrt{3}} . \tag{37}$$

As we have stated in Paper III, the fact that the plasmon

and shear modes exhibit the same asymptotic behavior can be understood in two ways: First observe that in view of the neglect of direct thermal effects, Kohn's sum rule (which states that the frequency squares summed over the modes of an OCP have to equal the plasma frequency squared, irrespective of k) has to hold within the quasilocalization approximation. Consequently, (37) is the only value permitted since for infinitesimally short wavelengths there is no distinction between the two transverse (doubly degenerate) shear modes and the longitudinal plasma mode and ω_p^2 has to be shared equally among the three [14]. Second, for an infinitesimally short-wavelength oscillation, the oscillating particle samples its immediate neighborhood only and therefore its oscillation frequency is identical to that of an isolated particle in the center of a uniform cloud of opposite background charge [15]: this frequency is $\omega_p/\sqrt{3}$.

We have calculated $\mathcal{D}_T(\mathbf{k})$ from (8) and (22) for arbitrary values of k using numerical data for the structure function $S(k)=1+ng(k)$ obtained by Rogers *et al.* [16] through the hypernetted-chain equation modified by the hard-sphere bridge function. The dispersion curve generated by this $\mathcal{D}_T(\mathbf{k})$ is displayed as the lower branch in Fig. 1 for the supercooled liquid state at $\Gamma=225$ and in Fig. 2 for $\Gamma=20$, 50, 100, and 150, and 225. We see that the acoustic part of the shear mode is not restricted to the small ka values assumed in the derivation of (35), but persists, in fact, up to $ka\sim 1.5$–2. With increasing k, $\omega(\mathbf{k})$ increases to a maximum whose value as $\Gamma\to\Gamma_m$ is $\omega_{\max}=0.639\omega_p$ at $ka=4.27$. Thereafter, $\omega(\mathbf{k})$ descends through a series of oscillations to the asymptotic value (37). The oscillations, because they originate from oscillations in the structure function $S(k)$, because more and more pronounced with increasing Γ (Fig. 2). The wave-number positions of the first and successive maxima (minima) in the shear-mode frequency coincide with the wave-number positions of the first (second) and successive minima (maxima) in the plasmon frequency.

There is a close affinity between the shear mode of the strongly coupled OCP and the acoustic phonons of the bcc Wigner lattice. While drawing up a comparison, however, one should bear in mind the inherent difference generated in the mode structure by the anisotropy of the crystal. In the crystal lattice, in addition to the dispersion being dependent on the direction of the propagation, the degeneracy of the two acoustic modes is lifted and their polarization is not purely transverse. With this proviso in mind, one can compare the shear velocity obtained from Eq. (36) for $\Gamma\to\Gamma_m$ with those calculated by Caldwell-Horsfall and Maradudin [5] in a few selected directions. This is shown in Table I. Apparently, there is a rather wide spectrum of shear velocities in the lattice: the shear velocity of the liquid falls roughly in the middle range. There is, however, a more direct way to demonstrate the close similarity of the excitations in the two systems that are masked by the lattice anisotropy. Averaging over all possible lattice orientations eliminates the anisotropy and serves as the proper basis for comparison. In a recent paper [14], one of us has shown that as $\Gamma\to\Gamma_m$, to $O(k^2)$ the OCP plasmon mode frequency squared tends to the angle-averaged optical (plasmon) frequency squared of the lattice in the same way as the correlation energies of the two systems approach each other. By virtue of the Kohn sum rule that applies both to the plasma and to the crystal, the same statement holds true for the acoustic shear mode: that is, if a proper average is taken over the values in Table I, the agreement between the two systems is as good as it is for the correlation energies. This is shown in the last entry of the table.

For finite k values, the comparison is further hindered by the lack of available calculational data on phonon dispersion in an arbitrary direction in the lattice. However, if (somewhat arbitrarily) we choose the [111] direction to represent the lattice, a good qualitative agreement can be found. Toya [6] and Sham [6] calculated the dispersion for sodium in this direction; their calculations have been corroborated by the experimental data of Woods *et al.* [7]. (For the metallic sodium, the dispersion is, of course, different from the dispersion in the pure Wigner lattice; nevertheless, for moderately large k values the difference for the transverse mode becomes

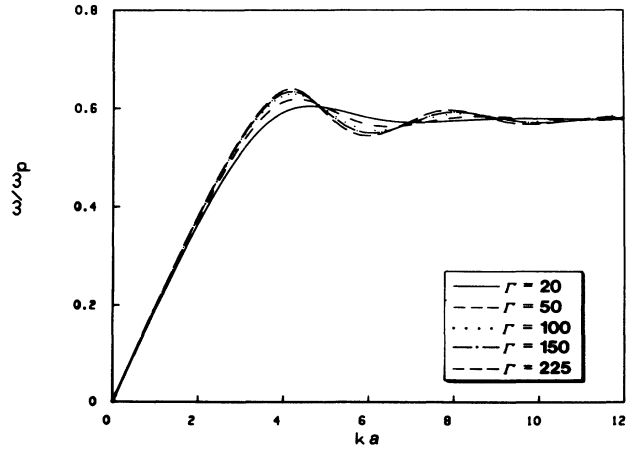

FIG. 2. Transverse shear-mode dispersion [calculated from QLC Eq. (32)] for $\Gamma=20$, 50, 100, 150, and 225.

TABLE I. Comparison of shear velocities in the three-dimensional Wigner crystal with the shear-mode velocity of the Coulomb liquid in the $\Gamma\to\Gamma_m$ limit as calculated in this work.

Direction		$V_0/\omega_p a$
		0.200
Ref. [5] [100]		0.247
[110]	I	0.247
	II	0.090
[111]		0.160
[210]	I	0.247
	II	0.173
[211]	I	0.208
	II	0.167
[221]	I	0.208
	II	0.118
Angle average		0.199

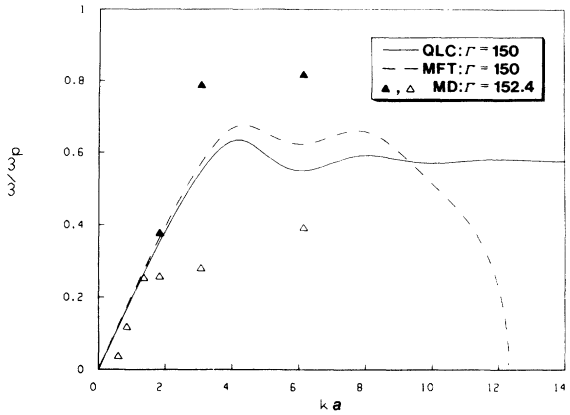

FIG. 3. Comparison of Hansen, McDonald, and Pollock (Ref. [8]) MD shear-mode data (triangle data points) for $\Gamma=152.4$ with the QLC Eq. (32) (solid line) and MFT Eq. (40) (dashed line) shear-mode dispersion curves for $\Gamma=150$.

negligible, as can be seen through comparison with Clark's [4] data.) The first intersection of the optic and acoustic phonons occurs at the $(\frac{1}{2},\frac{1}{2},\frac{1}{2})$ point corresponding to $ka=2.68$; this can be compared with the first intersection of the liquid-phase plasmon and shear modes in Fig. 1: for $\Gamma=225$, it occurs at $ka=3.29$. The second intersection occurs at the (1,1,1) point at $ka=5.36$; the corresponding value in Fig. 1 is 5.15 for $\Gamma=225$. As an aside, the liquid-phase plasmon and shear mode curves always intersect at the same frequency $\omega=\omega_p/\sqrt{3}$: this is to be expected, since by definition, the expressions (28) and (32) are equal at these intersections whence from (22), $\mathcal{D}_L(\mathbf{k},\Gamma)=-\frac{2}{3}$ and $\mathcal{D}_T(\mathbf{k},\Gamma)=\frac{1}{3}$.

We have compared our $\Gamma=150$ dispersion curve with the $\Gamma=152.4$ Hansen-McDonald-Pollock [8] MD shear data (Fig. 3). Agreement between the two is fairly satisfactory for ka values up to 1.384. The MD experiments reveal, however, that at higher ka values, the shear mode splits into a high-frequency mode and a low-frequency mode. Our QLC dispersion curve passes roughly midway between the two. Bosse and Kubo [17] have suggested that this splitting originates from plasmon–shear-mode interaction. If this conjecture is correct, then the absence of mode-mode interactions in the QLC liquid state formalism sheds some light on why this formalism would generate one and only one (doubly degenerate) shear-mode dispersion curve.

IV. SHEAR-MODE DISPERSION WITH DIRECT THERMAL EFFECT INCLUDED

In addition to the "indirect" thermal effect encountered through the temperature dependence of the correlation function, the particles in the liquid state undergo a slow change of the position of their equilibrium quasisites, which we have referred [1–3] to as the direct thermal effect. The QLC theory developed and employed in Secs. II and III ignores this effect, which becomes less and less significant as Γ increases toward Γ_m. Similar to what occurs in the dispersion of the longitudinal plasmon mode [2], the influence of the direct thermal motion on the transverse shear-mode dispersion is expected to be of the order kv_{thermal}. In contrast to the longitudinal mode, however, the thermal diffusion and migration is expected to affect the behavior of the transverse mode in a more fundamental way. The main manifestation of this is the disappearance of the shear mode for $k<k_{\min}$, where $k_{\min}$ is determined by v_{thermal}. Also, more akin to the modification experienced in the case of the plasmon mode, one expects the pronounced oscillations in the dispersion relation to be damped out and the mode to cease to propagate for $k>k_{\max}$ because of strong Landau damping.

At the present time we have no *ab initio* approach to incorporate the direct thermal effect into the theory. However, a phenomenological treatment, through MFT-type reformulation of the transverse element ϵ_T of the dielectric tensor $\underline{\epsilon}(\mathbf{k}\omega)$ can be carried out. The result is given below, in terms of a transverse local-field correction $F(\mathbf{k}\omega)$, which is analogous to the customary (longitudinal) local-field correction $G(\mathbf{k}\omega)$ widely used in the theory of the correlated electron gas and also introduced in our previous papers [2,3]:

$$\alpha_T(\mathbf{k}\omega)=\frac{\alpha_{T0}(\mathbf{k}\omega)}{1-F(\mathbf{k}\omega)\alpha_{T0}(\mathbf{k}\omega)}\ , \tag{38}$$

where $\alpha_{T0}(\mathbf{k}\omega)$ is the transverse random-phase approximation polarizability

$$\alpha_{T0}(\mathbf{k}\omega)=-\frac{\omega_p^2}{n\omega}\int d^3v\frac{F^{(0)}(v)}{\omega-\mathbf{k}\cdot\mathbf{v}+io}\ , \tag{39}$$

with $F^{(0)}(v)=n(\beta m/2\pi)^{3/2}\exp[-\beta m v^2/2]$.

Even though there is no unique prescription for the phenomenological construction of $F(\mathbf{k}\omega)$, there are certain obvious criteria whose satisfaction for the resulting $\alpha_T(\mathbf{k}\omega)$ is expected, such as the recovery of (20) in the $v_{\text{thermal}}=0$ limit and the satisfaction of the transverse third-frequency-moment sum rule—including the hitherto neglected thermal contribution. Thus we choose $F(\mathbf{k}\omega)=-\mathcal{D}_T(\mathbf{k})$.

Our interest is in the MFT reformulation of the shear-mode dispersion. Therefore, since the index of refraction $kc/\omega\gg1$ for this mode, it is sufficient to work with the approximate dispersion relation $\epsilon_T^{-1}(\mathbf{k}\omega)=0$, i.e.,

$$1+\alpha_{T0}(\mathbf{k}\omega)\mathcal{D}_T(\mathbf{k})=0\ . \tag{40}$$

In the wave-number domain $k>\omega_p/c$ [i.e., at wave numbers $(ka)^2\gg3\Gamma/(\beta mc^2)$], where the shear mode is physically viable, an analysis of Eq. (40) reveals (i) that there is a minimum Γ value $\Gamma_{\min}=9.41$ below which no transverse shear modes can exist, and (ii) the existence of a high-k cutoff $k_c\approx\sqrt{\Gamma}/a$, where the shear-mode oscillation frequency is zero; the shear mode ceases to exist at wave numbers $k>k_c$.

For $\Gamma>\Gamma_{\min}=9.41$ and $3\Gamma/(\beta mc^2)\ll(ka)^2\ll1$, one obtains the MFT acoustic shear-mode frequency

$$\text{Re}\omega(\mathbf{k})=A(\Gamma)kV_0\ , \tag{41}$$

where V_0 is given by (36); the small MFT correction in

$$A(\Gamma)=\frac{1}{\sqrt{2}}\left[1+\left[+\frac{30}{\beta|E_c(\Gamma)|}\right]^{1/2}\right]^{1/2}, \quad (42)$$

of course, becomes less and less significant with increasing Γ. Figure 4 indicates that the acoustic part of the MFT shear mode is not restricted to small ka values, but persists, like its QLC counterpart, up to $ka \sim 1.5$–2. The most significant feature of the MFT description is the large-k cutoff $k_c a \approx \sqrt{\Gamma}$, beyond which the shear mode ceases to exist. Strong Landau damping keeps the shear wave from propagating even at wave numbers in the domain $k_{\max}(\Gamma) < k < k_c$: in this domain, the Landau damping rate $\gamma(\mathbf{k}) \equiv \mathrm{Im}\omega(\mathbf{k})$ exceeds the shear-mode oscillation frequency $\mathrm{Re}\omega(\mathbf{k})$ [$k_{\max}$ is the value of k where $\gamma(\mathbf{k}) = \mathrm{Re}\omega(\mathbf{k})$; see Fig. 5].

The MFT fails to provide the expected suppression of the shear mode for $k < k_{\min}$: the present formulation with a frequency independent $F(\mathbf{k})$ is tantamount to a *static* mean-field theory, which is incapable of producing the diffusional damping mechanism required for the dissipation of the low-k modes. Only a more sophisticated dynamical mean-field theory (perhaps along the line of our earlier work [18,19]) would be able to do this. Nevertheless, an order-of-magnitude estimate for $k_{\min}$ can be based on the assumption that the shear mode disappears when the diffusion time (τ_D) is shorter than the oscillation period, i.e., when $\omega\tau_D \leq 1$. τ_D can be estimated as $\tau_D \approx \lambda^2/D$, where λ is a characteristic migration distance of a particle from its quasisite position sufficient to disrupt the generation of the restoring shear force: D is the self-diffusion coefficient. We estimate λ as $a/4$ (note that the Lindeman melting criterion requires [20] only $\lambda = a/5$). D for strong coupling has been inferred from MD data by Hansen, McDonald, and Pollock [8]: $D \approx 3(\omega_p a^2/\Gamma^{1.3})$. This condition combined with Eq. (35) leads to $k < k_{\min}$ with $k_{\min} a \approx 240/\Gamma^{1.3}$. Thus our dispersion curves should be considered unreliable below this $k_{\min}$ value. It is interesting to observe how the combination of this estimate for $k_{\min}$ with the previously noted $k_{\max} < k_c \approx \sqrt{\Gamma}/a$ brackets the physically viable propagation domains to smaller and smaller regions in k space as Γ decreases.

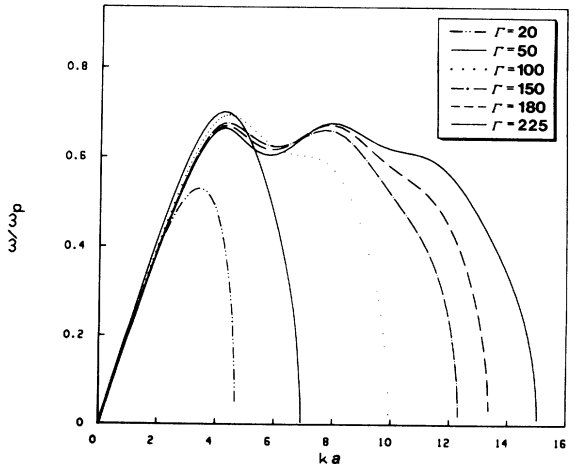

FIG. 4. Transverse shear-mode dispersion [calculated from MFT Eq. (40)] for $\Gamma = 20$, 50, 100, 150, 180, and 225.

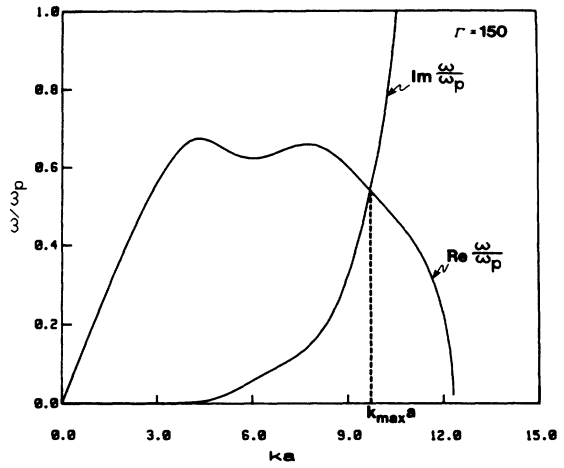

FIG. 5. MFT shear-mode oscillation frequency $\mathrm{Re}\omega(\mathbf{k})/\omega_p$ and Landau damping rate $\gamma(\mathbf{k})/\omega_p \equiv \mathrm{Im}\omega(\mathbf{k})/\omega_p$ [calculated from Eq. (40)] for $\Gamma = 150$.

In Fig. 3 we have compared the $\Gamma = 152.4$ Hansen-McDonald-Pollock MD data [8] both with the QLC and MFT dispersion curves calculated for $\Gamma = 150$. Agreement between either of the calculated curves and the MD data is fairly satisfactory in the acoustic domain. Recalling the splitting of the MD data into two shear modes at higher ka values, both the MFT and the QLC curves pass between the two, but the MFT curve appears to favor the higher-frequency mode. The MFT calculations suggest that shear waves should be too heavily Landau damped to propagate at wave numbers $k \geq k_{\max}(\Gamma = 152.4) \approx 9.77/a$. Unfortunately, the disappearance of the shear mode at large k was not tested in the Ref. [8] MD experiments since the investigators did not go beyond $ka = 6.256$. Neither can one draw any conclusion from the MD data concerning the validity of the estimate for $k_{\min}$: $k_{\min} a(\Gamma = 152.4) = 0.35$, while the lowest ka value in the computer simulation was 0.619. In anticipation of the following paper, one may point out, however, that the 2D numerical experiments of Totsuji and Kakeya [21] give good agreement with the calculated $k_{\max}$ and reasonable agreement with the estimated $k_{\min}$ values.

V. CONCLUSIONS

In this paper we have calculated the full dielectric-response tensor and analyzed the transverse mode, in particular the shear-mode behavior of the strongly coupled 3D OCP. The derivations of the polarizability formulas (20) and (21) and the subsequent reformulation into the transverse mean-field-theory expressions (38) are based on the quasilocalization-charge (QLC) model of the system. This approach is appropriate for taking account of the strong correlations between the particles, which is the crucial factor in enabling the system to maintain shear waves.

Our analytical and numerical calculations have been carried out at finite wave numbers and over a coupling range $20 \leq \Gamma \leq 225$, extending into the domain of possible supercooled states. In the physically most interesting wave-number domain $kc \gg \omega_p$, the QLC shear-mode dispersion is given by Eqs. (32), (35), and (37). For the very long-wavelength ($kc < \omega_p$) domain, the shear-mode dispersion assumes a quadratic behavior given by Eq. (34). Our numerical calculations indicate that the acoustic domain is not at all restricted to the small ka values assumed in the derivation of (35) but rather it extends up to ka values of 2. As Γ increases and approaches the crystallization limit Γ_m, the QLC results are in good qualitative agreement with the calculated and measured acoustic-phonon dispersions in the respective Wigner crystals; in the small-k limit, where analytic comparison is possible, the agreement with calculated results is excellent.

We have incorporated the direct thermal effects in the QLC formalism by generating a static-mean-field theory, resulting in Eq. (38). As a consequence, a more complete and reliable description of the shear mode has become possible. No shear wave exists beyond a critical k value $k_{\max}(\Gamma)$; for $k > k_{\max}$ the wave becomes too heavily Landau damped to propagate. As to $k_{\min}$, neither the QLC model nor the static MFT approach are able to account for the diffusion-type damping that is responsible for the breakdown of the shear-mode propagation as $k \to 0$. Nevertheless, a simple estimate, based on the physical picture inherent in the QLC model, provides a value for $k_{\min}$ below which no propagation is expected and whose value is compatible with MD data. There also exists a minimum value of Γ, $\Gamma_{\min}$, below which the transverse shear mode ceases to exist; we calculate $\Gamma_{\min} = 9.41$; this value is probably an underestimate (too high Γ), since the limitation coming from the low-k breakdown of propagation would further inhibit the existence of the shear mode.

We have compared our $\Gamma = 150$ $3D$ QLC and MFT transverse shear-mode dispersions with the $\Gamma = 152.4$ Hansen-McDonald-Pollock MD shear data (Fig. 3). Agreement between theory curves and computer experiments is quite satisfactory in the acoustic domain up to $ka = 1.384$. At higher ka values, however, the MD data indicate a splitting into a high-frequency mode and a low-frequency mode. The QLC theory curve passes roughly midway between the two modes. So does the MFT curve, but it appears to favor the high-frequency mode. The explanation for this behavior is probably to be sought in mode-mode interaction, whose inclusion in the model requires further work.

ACKNOWLEDGMENTS

This work has been partially supported by the National Science Foundation Grant Nos. ECS-8713628, PHY-9115695, ECS-8713337, and PHY-9115714.

[1] G. Kalman and K. I. Golden, Phys. Rev. A **41**, 5516 (1990).
[2] K. I. Golden, G. Kalman, and P. Wyns, Phys. Rev. A **41**, 6940 (1990).
[3] M. Minella, G. Kalman, K. I. Golden, and P. Carini (unpublished).
[4] C. B. Clark, Phys. Rev. **109**, 1133 (1958).
[5] R. A. Caldwell-Horsfall and A. A. Maradudin, J. Math. Phys. **1**, 395 (1960).
[6] L. J. Sham, Proc. R. Soc. London, Ser. A **283**, 33 (1965); T. Toya, J. Res. Inst. Catal. Hokkaido Univ. **6**, 161, 183 (1958); S. H. Vosko, R. Taylor, and G. H. Keech, Can. J. Phys. **43**, 1187 (1965); S. K. Joshi and A. K. Rajogopal, in *Solid State Physics Advances in Research and Applications,* edited by F. Seitz, D. Turnbull, and H. Ehrenreich (Academic, New York, 1968), Vol. 22, p. 160.
[7] A. D. B. Woods, B. N. Brockhouse, R. H. March, A. T. Steward, and R. Bowers, Phys. Rev. **128**, 1112 (1962).
[8] J. P. Hansen, I. R. McDonald, and E. L. Pollock, Phys. Rev. A **11**, 1025 (1975).
[9] K. I. Golden and G. Kalman, Phys. Lett. A **149**, 401 (1990).
[10] G. Kalman and R. Genga, Phys. Rev. A **33**, 604 (1986).
[11] G. S. Stringfellow, H. E. DeWitt, and W. L. Slattery, Phys. Rev. A **41**, 1105 (1990).
[12] R. W. Shaw, J. Phys. C **3**, 1140 (1970).
[13] G. Niklasson, Phys. Rev. B **10**, 3052 (1974).
[14] G. Kalman, Phys. Lett. A **141**, 433 (1989).
[15] We are grateful to P. Bakshi, to whom this observation is originally due.
[16] F. J. Rogers, D. A. Young, H. E. DeWitt, and M. Ross, Phys. Rev. A **28**, 2990 (1983); H. E. DeWitt (private communication).
[17] J. Bosse and K. Kubo, Phys. Rev. Lett. **40**, 1660 (1978); Phys. Rev. A **18**, 2337 (1978).
[18] K. I. Golden and G. Kalman, Phys. Rev. A **19**, 2112 (1979).
[19] Z. C. Tao and G. Kalman, Phys. Rev. A **43**, 973 (1991).
[20] T. E. Faber, *Theory of Liquid Metals* (Cambridge University Press, Cambridge, England, 1972).
[21] H. Totsuji and H. Kakeya, Phys. Rev. A **22**, 1220 (1980).